Molecular Modeling and Solid-State NMR of Short-Chain Molecules in Dianin's Compound and Zeolite 5A

Eduardo Zaborowski,[†,‡] Herbert Zimmermann,[§] and Shimon Vega*[,†]

Contribution from the Department of Chemical Physics, Weizmann Institute of Science, Rehovot, Israel, and Max-Planck-Institut für Medizinische Forschung, Heidelberg, Germany

Received March 12, 1998

Abstract: We have investigated the reorientational mobility of *n*-hexane and *n*-pentanol guest molecules in Dianin's compound and in zeolite 5A by molecular mechanics/dynamics calculations (MM/MD) and temperature-dependent solid-state ^{2}H NMR. To choose the proper motional models for the different host−guest systems, MM calculations were first performed and minimum-energy structures for the compounds were established. The calculations were performed on a crystallographic unit cell, with periodic boundary conditions to minimize edge effects. MD methods were then applied to the minimized structures and provided an insight into the different dynamic modes experienced by the guest molecules in their host cages. Several structural parameters of the host−guest systems were monitored for a total simulation period of up to 100 ps both at low temperature (77 K) and high temperature (300 K). ^{2}H NMR spectra of perdeuterated and specifically deuterated guest molecules in their inclusion compounds were acquired as a function of temperature. After detection the observed line shapes were analyzed in terms of motional models, taking into account experimental parameters and the results of the MD calculations. The solid-state ^{2}H NMR showed a very high degree of agreement with the results of the molecular modeling calculations.

1. Introduction

1.1. Inclusion Compounds. The chemical structures of inclusion compounds are unique in the sense of their capability of enclosure. The interaction between host and guest molecules in these materials is governed by chemical and physical forces and can be considered as a model for the understanding of enzyme−substrate systems.[1] The static properties of host−guest crystalline compounds have been studied by several experimental techniques such as X-ray crystallography[2] and differential thermal analysis (DTA).[3] The characterization of the vibrational, rotational, and translational degrees of freedom that guest molecules experience upon inclusion has been done with the help of spectroscopic methods such as IR and Raman.[4] NMR spectroscopy can provide information on molecular motions of these systems, with time scales on the order of $10-10^{10}$ Hz. Several NMR studies have shown the power of this approach to investigate the dynamic properties of molecules in host−guest complexes.[5−7] We present here our study of molecules included in Dianin's inclusion compound and in zeolite 5A.

Dianin's inclusion compound is an organic clathrate in which a large group of different small molecules can be included with the ratio between guest and host molecules fixed by the size of the guest.[8] The length of the cages as determined by Flippen et al. is ≈11 Å, and the diameter is ≈6.3 Å at their widest part and ≈4.2 Å at their narrowest part. Furthermore, these values are almost unaffected by the type and size of the guest molecules.[9] The structure and dynamics of several Dianin's inclusion compounds have been studied by solid-state NMR. Among others, we direct the reader to the ^{13}C and ^{129}Xe works of Ripmeester and collaborators,[5,10] to the single-crystal ^{2}H NMR studies of Bernhard et al.,[11] and to our own previous studies of *p*-xylene and *o*-xylene guest adducts that combined powder/single-crystal ^{2}H NMR and energy calculations.[12−14]

Zeolite 5A has α cages with dimensions similar to those of the Dianin's compound (≈11.4 Å in diameter)[15] so that guest molecules of similar size can be included in both compounds. NMR has contributed in many cases to improving the understanding of the structure of the zeolites[16,17] and the properties

† Weizmann Institute of Science.

‡ Current address: Department of Molecular Biology, The Scripps Research Institute, La Jolla, CA.

§ Max-Planck-Institut.

(1) Powell, H. M. In *Inclusion Compounds*; Atwood, J. L., Davies, J. E. D., MacNicol, D. D., Eds.; Academic Press: London, 1984; Vol. 1.

(2) Andretti, G. D. In *Inclusion Compounds*; Atwood, J. L., Davies, J. E. D., MacNicol, D. D., Eds.; Academic Press: London, 1984; Vol. 3.

(3) Parsonage, N. G.; Staveley, L. A. K. In *Inclusion Compounds*; Atwood, J. L., Davies, J. E. D., MacNicol, D. D., Eds.; Academic Press: London, 1984; Vol. 3.

(4) Davies, J. E. D. In *Molecular Spectroscopy*; Barrow, R. F., Long, D. A., Sheridan, J., Eds.; The Chemical Society: London, 1978; Vol. 5.

(5) Ripmeester, J. A. *J. Inclusion Phenom.* **1983**, *1*, 87−91.

(6) Kustanivich, I.; Fraenkel, D.; Luz, Z.; Vega, S.; Zimmermann, H. *J. Phys. Chem.* **1988**, *92*, 4134−4141.

(7) Vold, R. R. In *Nuclear Magnetic Resonance Probes of Molecular Dynamics*; Tycko, R., Ed.; Kluwer Academic Publishers: Dordrecht, The Netherlands, 1994.

(8) Baker, W.; Floyd, A. J.; McOmie, J. F. W.; Pope, G.; Weaving, A. S.; Wild, J. H. *J. Chem. Soc.* **1956**, 2010−2017.

(9) Flippen, J. L.; Karle, J.; Karle, I. L. *J. Am. Chem. Soc.* **1970**, *92*, 3749−3755.

(10) Lee, F.; Gabe, E.; Tse, J. S.; Ripmeester, J. A. *J. Am. Chem. Soc.* **1988**, *110*, 6014−6019.

(11) Bernhard, T.; Zimmermann, H.; Haeberlen, U. *J. Chem. Phys.* **1990**, *92*, 2178−2186.

(12) Zaborowski, E.; Vega, S. *Mol. Phys.* **1993**, *78*, 703−732.

(13) Speier, P.; Prigl, G.; Zimmermann, H.; Haeberlen, U.; Zaborowski, E.; Vega, S. *Appl. Magn. Reson.* **1995**, *9*, 81−102.

(14) Zaborowski, E.; Vega, S.; Speier, P.; Zimmermann, H.; Haeberlen, U. *Mol. Phys.* **1997**, *91*, 1083−1096.

(15) Breck, D. W. *Zeolite Molecular Sieves*; Robert E. Krieger Publishing Company: Malabar, FL, 1984.

(16) Engelhardt, G.; Michel, D. *High-Resolution Solid State NMR of Silicates and Zeolites*; John Wiley & Sons: New York, 1987.

(17) Fyfe, C. A.; Feng, Y.; Grondey, H.; Kokotailo, G. T.; Gies, H. *Chem. Rev.* **1991**, *91*, 1525−1543.

S0002-7863(98)00831-2 CCC: $15.00
Published on Web 08/05/1998

of adsorbed molecules. Examples of these contributions are the ^{29}Si CP-MAS studies of Brönsted acid sites and surface structure carried out by Blumenfeld et al.,[18] the ^{13}C analysis of the dynamics of benzene adsorbed on Ca−LSX zeolite done by Wilhelm et al.,[19] and the comparative study of the dynamics of benzene in siliceous faujasite by ^{2}H NMR and molecular dynamics done by Bull et al.[20] Molecular simulation methods have also contributed, in works such as those of Catlow[21] and Smit.[22]

1.2. Energy Calculations and ^{2}H Solid-State NMR. In the study, we have investigated the reorientational mobility of guest molecules in their hosts by molecular mechanics and molecular dynamics. Over the past decade the fast growth of molecular modeling as a research tool in biology, medicine, and materials research has been tightly coupled to the advent of the supercomputer and to advances in applied and computational mathematics. In molecular mechanics (MM) calculations one uses the potential-energy functions to compute the forces exerted on atoms and different algorithms to change the atom's positions to minimize these forces. The result is a structure with minimized energy. Molecular dynamics (MD) uses Newton's equations of motion to move the atoms in response to the applied forces. The result is a description of how the atomic positions change with respect to time.

A large number of so-called force fields (potential-energy functions) for use with polyatomic systems have become available in recent years.[23−26] A typical potential energy function is the sum of several interactions and can be written schematically in the form:

$$V_T = \sum_{\substack{1,2\\ \text{pairs}}} \frac{1}{2} K_b (b - b_0)^2 + \sum_{\substack{\text{bond}\\ \text{angles}}} \frac{1}{2} K_\theta (\theta - \theta_0)^2 + \sum_{\substack{\text{dihedral}\\ \text{angles}}} K_\phi [1 + \cos(n\phi - \delta)] + \sum_{\substack{\text{nonbonded}\\ \text{i,j pairs}}} 4\epsilon_{ij}\left[\left(\frac{\sigma_{ij}}{r}\right)^{12} - \left(\frac{\sigma_{ij}}{r}\right)^{6}\right] + \frac{1}{\epsilon}\frac{q_i q_j}{r}$$

composed of (1) a harmonic restoring force between bonded atoms, where b, K_b, and b_0 are the bond length, the bond-stretching force constant, and the equilibrium distance parameter, respectively, (2) a deformation term for the angle between three neighboring atoms, where θ, K_θ, and θ_0 are the bond angle, the angle bending force constant, and the equilibrium value parameter, (3) a dihedral torsional potential, where ϕ, K_ϕ , n, and δ are a dihedral angle, its force constant, its multiplicity, and its phase, and (4) nonbonded interactions between separated atoms, where r, ϵ_{ij}, σ_{ij}, q_i, and ϵ are the nonbonded distance, the dispersion well-depth, the Lennard-Jones diameter, the charge, and a dielectric parameter.

In addition to these calculations, we have performed temperature-dependent solid-state ^{2}H NMR of deuterated guest molecules in their inclusion compounds. The NMR spectrum of a single $I = 1$ nucleus has two allowed transitions, at $\omega_0 \pm \omega_Q$, where ω_0 is the Larmor frequency and ω_Q is the quadrupolar frequency given by

$$\omega_Q = \frac{3}{2}\frac{e^2Qq}{4I(2I-1)\eta}(3\cos^2\theta - 1 - \eta_Q \sin^2\theta \cos 2\phi)$$

Here θ and ϕ are the polar angles of the magnetic field vector in the principal axis system (PAS) of the electric field gradient (EFG) tensor, which is fully defined by two parameters: eq (the electric field gradient) and η_Q (the asymmetry parameter). The value e^2Qq/η is called the nuclear quadrupolar coupling constant, NQCC. In the case of a single crystal this gives rise to a doublet in the NMR spectrum and in a powder sample to a distribution of lines known as a powder pattern, with sharp features at the frequencies equal to the values of the principal tensor components in the PAS frame. For $\eta_Q = 0$, the components with $\theta = 0°$ and 90° are called parallel and perpendicular. The splitting between the two $\theta = 90°$ components is called the *quadrupolar splitting* and has a value that is 3/4 of the NQCC. The resulting deuterium NMR line shapes are clearly very sensitive to molecular motions, especially when their rates are on the order of the line width of the static NMR spectrum.[27,28]

2. Experimental Section

2.1. Materials and Methods. Dianin's inclusion compounds were prepared by recrystallization of the guest-free compound from a solution of the desired labeled guest molecules. Zeolite 5A inclusion compounds were prepared by (1) activation of the zeolite for 24 h at a temperature above 300 °C, with the pressure kept below 10^{-5} Torr and (2) adsorption of a known amount of guest compound on the activated zeolite at low pressure ($<10^{-5}$ Torr), while keeping the zeolite at liquid nitrogen temperature. The amount of the guest compound used was calculated to yield one molecule per α cage. NMR spectra acquired with half the amount of guests gave absolutely the same line shape, with reduced signal-to-noise ratios.

2.2. ^{2}H NMR. ^{2}H NMR spectra were measured on a Bruker DSX-300 AVANCE spectrometer at a frequency of 46.07 MHz, with a home-built low-temperature probe that fits into a continuous-flow cryostat. The temperature, sensed close to the rf coil, was controlled to be less than ±0.1 K. Solid-echo ($90^\circ_x-\tau-90^\circ_y-\tau-$ACQ) sequences were used with 90° pulses of typically 2.0−3.0 μs and a τ value between the 90° pulses of 20 μs. This τ value was changed to investigate its effect on the dynamic line shapes. Spin−lattice relaxation times (T_1) were measured with a solid-echo inversion−recovery sequence. The number of scans was typically 5000−20000. Experimental NMR data were processed with the standard Bruker program XWIN-NMR. The observed line shapes were analyzed in terms of motional models, taking into account the measured ^{2}H relaxation parameters and all other relevant experimental conditions. Simulation of the deuterium line shapes was carried out with in-home written programs for dynamics of deuterium nuclei in powders. They calculate the orientation-dependent contribution of a single group of exchanging nuclei (one crystallite) and then integrate over typically 6000 crystallites oriented uniformly in all possible directions.

2.3. Molecular Mechanics and Molecular Dynamics Calculations. Energy calculations were performed using the open force field (OFF) module of the Cerius^2 program package developed by BIOSYM/

(18) Blumenfeld, A. L.; Coster, D.; Fripiat, J. J. *J. Phys. Chem.* **1995**, *99*, 15181−15191.
(19) Wilhelm, M.; Firouzi, A.; Favre, D. E.; Bull, L. M.; Schaefer, D. J.; Chmelka, B. F. *J. Am. Chem. Soc.* **1995**, *117*, 2923−2924.
(20) Bull, L. M.; Henson, N. J.; Cheetham, A. K.; Newsam, J. M.; Heyes, S. *J. Phys. Chem.* **1993**, *97*, 11776−11780.
(21) Catlow, C. R. A.; Freeman, C. M.; Vessal, B.; Tomlinson, S. M.; Leslie, M. *J. Chem. Soc., Faraday Trans.* **1991**, *87*, 1947−1950. Catlow, C. R. A.; Bell, R. G. *Solid State Ionics* **1994**, *70*, 511−517.
(22) Smit, B.; Siepmann, J. I. *Science* **1994**, *264*, 1118−1120.
(23) Weiner, S. J.; Kollman, P. A.; Nguyen, D. T.; Case, D. A. *J. Comput. Chem.* **1986**, *7*, 230.
(24) Rappe, A. K.; Casewit, C. J.; Colwell, K. S.; Goddard, W. A., III; Skiff, W. M. *J. Am. Chem. Soc.* **1992**, *114*, 10024−10035.
(25) Mayo, S. L.; Olafson, B. D.; Goddard, W. A., III. *J. Phys. Chem.* **1990**, *94*, 8897−8909.
(26) Kao, J.; Allinger, N. L. *J. Am. Chem. Soc.* **1977**, *99*, 975.
(27) Spiess, H. W. *Colloid Polym. Sci.* **1983**, *261*, 193−209.
(28) Griffin, R. G. *Methods Enzymol.* **1981**, *72*, 108.

Molecular Simulations. The OFF module offers several force fields for use with organic molecules (UFF, DREIDING, CFF91/95, CVFF family) and zeolites (Burchart, BKS). We chose to use the Burchart force field for the zeolites because OFF has a mixed Burchat−DREIDING force field suitable for the energy calculation of zeolite−organic sorbate interactions. For the sake of comparison, the DREIDING force field was also chosen for the Dianin's inclusion compounds. For these compounds, the CVFF(950) force field was used to check the effect of using a force field more specialized in organic molecules. We direct the interested reader to the Cerius[2] documentation and to the original references of the CVFF(950),[29] DREIDING,[25] and Burchart[30] force fields.

Atom's force field types were automatically assigned by each of the force fields. In the case of deuterium atoms, the atomic masses of the specific labeled atoms were set to 2.014 amu. Terms for the energy expressions were automatically set up according to the force field used, and the long-range interactions were calculated by the Ewald summation method and excluded van der Waals/Coulombic interactions between directly bonded (1−2 interactions) atoms and between atoms bonded to a common atom (1−3 interactions). Atomic charges were set either manually or automatically by the force field or were calculated by the charge equilibration (Qeq) method.[31] MM methods were applied for the energy minimization of the periodic structures of the inclusion compounds. We used for the calculations one crystallographic unit cell, with periodic boundary conditions (PBC) to minimize edge effects. The periodic structures were minimized either with or without constraining the unit cell parameters (lengths and angles). There are several methods available for the minimization. We chose the Cerius[2] minimization module default method, which starts as steepest descent, followed by the adopted basis Newton−Raphson (ABNR) and quasi-Newton methods, and ends with the more accurate truncated Newton method. Other methods are available and well documented in the Cerius[2] manuals. MD was applied to the energy-minimized structures with a constant *NVT* method at low (77 K) and high (300 K) temperatures. The model exchanges heat with a heat bath to maintain a constant temperature through the noncanonical T_Damp method of Beredsen et al.,[32] with a relaxation time of 0.1 ps. The MD time steps were chosen to be 1 fs, and trajectory files were saved every 10−20 steps. MD was performed on one crystallographic unit cell, with PBC. Analysis of the trajectory data was done with the dynamics analysis module of Cerius[2] and in-home written programs. The motion of the molecules was probed by the position of their centers of mass, the orientation of the relevant C−D bonds, and the molecules' internal torsion angles.

A typical calculation consisted of separately minimizing the structures of the empty host crystal and of the guest molecule, minimizing the host−guest system for several different initial guest positions, and using MD to calculate the trajectory of a minimized host−guest structure for periods of 20−100 ps at different temperatures. The numbers of atoms involved in the calculations were 720 (unsolvated Dianin's compound), 774 (pentanol−Dianin's compound), 780 (hexane−Dianin's compound), 640 (empty zeolite 5A), 784 (pentanol−zeolite 5A), and 800 (hexane−zeolite 5A). The 100 ps simulations required approximately 50 h of CPU time with the force-field evaluation being done by two CPUs of our ORIGIN-2000 Silicon Graphics computer.

3. Results

3.1. Energy Minimization for the Empty Dianin's Compound and Zeolite 5A. The crystal structure for the Dianin's compound cage was taken from the X-ray data of the single crystals of ethanol and chloroform Dianin's compounds published by Flippen et al.[9] The cell parameters for ethanol, chloroform, and unsolvated[33] Dianin's compound are shown in Table 1.

Table 1. Cell Parameters for the Ethanol, Chloroform, and Empty Dianin's Inclusion Compounds from X-ray Data[9,34]

compound	*a*/Å	*b*/Å	*c*/Å	α/deg	*β*/deg	*γ*/deg
unsolvated	26.9400	26.9400	10.9400	90.0000	90.0000	120.0000
ethanol	26.9690	26.9690	10.9900	90.0000	90.0000	120.0000
chloroform	27.1160	27.1160	11.0230	90.0000	90.0000	120.0000

Table 2. Cell Parameters for Empty Dianin's Inclusion Compound after Energy Minimization

force field	*a*/Å	*b*/Å	*c*/Å	α/deg	*β*/deg	*γ*/deg
DREIDING[a]	27.7339	27.7339	10.9157	90.0000	90.0000	120.0000
CVFF(950)[a]	26.7899	26.7899	11.0614	90.0000	90.0000	120.0000

[a] VDW and electrostatic terms calculated by Ewald summation with a cutoff of 6 Å. Enlarging the distance to 10 Å caused a change of less than 0.1% in the cell parameters, with a large increase in computation time.

Beginning with the ethanol clathrate host structure, we let the lattice relax with the single constraint of the $R\bar{3}$ space group. The variable parameters were then *a* and *c* as well as the individual coordinates of the host atoms. Atomic partial charges were calculated by the charge equilibration method (Qeq) for the DREIDING force field and were set automatically by the CVFF(950) force field. The results are shown in Table 2.

The changes in the cell parameters were small, less than 3% for the DREIDING force field and less than 0.5% for the CVFF-(950). They were bigger in the crystal *x* and *y* directions than in the *z* direction as a result of the packing of the structure.

The isolated hexane and pentanol guest molecular structures were minimized with the same force fields, and the partial charges were set as described above. The result, as expected, was an all-trans configuration for both molecules, with known bond distances and angles.

For the calculations of the minimal energy structures of the Dianin's compounds, three guest molecules, each containing three cages, were included per unit cell. Each included molecule was placed with its center of gravity coinciding with the center of one of the cages and with different relative positions and orientations. Any change in the position of the center of mass of the guest molecule resulted in a prohibitive increase in energy. This increase is caused by the repulsive forces of the methyl groups at the bottlenecks of the cages and the hydroxyl groups at the top and bottom of the cages.

Calling CP the chain plane containing all carbon atoms in the all-trans configuration, the initial orientations of the guests were taken as follows: (1) all guests with CP perpendicular to the crystallographic *bc* plane, (2) one guest with CP perpendicular to the *bc* plane and the other two as in (1), (3) one guest with CP forming an angle of 30° with plane *bc* and two as in (1), (4) one guest with CP forming an angle of 60° with plane *bc* and two as in (1), and (5) one guest as in (1), one as in (2), one as in (3).

Before the minimization of the host−guest structure, all constrains were removed; namely, the space group was set to be *P*1 and all cell lengths and angles were allowed to vary. For the pentanol guest molecules an additional set of calculations

(29) Hagler, A. T.; Dauber, P.; Lifson, S. *J. Am. Chem. Soc.* **1979**, *101*, 5131−5141. Hagler, A. T.; Lifson, S.; Dauber, P. *J. Am. Chem. Soc.* **1979**, *101*, 5122−5130. Lifson, S.; Hagler, A. T.; Dauber, P. *J. Am. Chem. Soc.* **1979**, *101*, 5111−5121.

(30) Burchart, E. de Vos. Studies on Zeolites: Molecular Mechanics, Framework Stability and Crystal Growth. Ph.D. Thesis, Technische Universiteit Delft, 1992.

(31) Rappe, A. K.; Goddard, W. A., III. *J. Phys. Chem.* **1991**, *95*, 3358−3363.

(32) Berendsen, H. J.; Postma, J. P. O.; Gunsteren, W. I. v.; Niola, A. D.; Haak, J. R. *J. Chem. Phys.* **1984**, *81*, 3684.

(33) MacNicol, D. D. In *Inclusion Compounds*; Atwood, J. L., Davies, J. E. D., MacNicol, D. D., Eds.; Academic Press: London, 1984; Vol. 2.

Table 3. Cell Parameters for Empty Zeolite 5A after Energy Minimization

compound	*a*/Å	*b*/Å	*c*/Å	α/deg	*β*/deg	*γ*/deg
empty zeolite	24.8400	24.8400	24.8400	90.0000	90.0000	90.0000
scaled charges	24.5888	24.5887	24.5887	90.0000	90.0000	90.0000
nonscaled charges	24.5455	24.5453	24.5453	90.0000	90.0000	90.0000

was performed, with the same orientations as above, but with one of the guests "upside down".

The crystal structure for the dehydrated zeolite 5A was taken from the studies of Seff and Shoemaker.[34] No Al−O−Al groups were allowed to exist. There are four Na^+ and four Ca^{2+} cations per cage, and their positions were chosen to be as follows. If one visualizes a cage to be a truncated cube, the cations are located at the proximity of the cube vertexes (see Figure 6), close to the plane of the S6R windows. We chose to position each type of cation in a tetrahedral arrangement so that each cation had as its next nearest neighbor a cation of the other type. To check the effect of the calculated (Qeq) values of the charges, we also performed minimizations with the electrostatic charges scaled by 0.75. The results are shown in Table 3.

Both minimizations showed a contraction of less than 1% in the cell length. When compared to the original structure, the cations' (Ca^{2+} and Na^+, respectively) positions changed mainly in the {111} directions, by 1.0−1.5 and 0.6−0.9 Å for the nonscaled charges and by 1.2−1.6 and 0.7−0.8 Å for the scaled charges. These values are an indication of the expected mobility of these cations in the zeolite structure.

For the energy minimization of the guest−zeolite systems, we considered one unit cell consisting of eight cages ($2 \times 2 \times 2$). Either one guest molecule was included in one of the cages or eight molecules were included, one in each cage. Each included molecule was placed initially with its center of gravity coinciding with the center of one of the cages. The long molecular axis was oriented pointing in the direction of one of the channels interconnecting the cages, running in the {001} directions.

3.2. Energy Minimization of Dianin's Compounds with Short Chains. 3.2.1. *n*-Hexane−Dianin's Compound. Minimization with the two different force fields showed slightly different results. The cell parameters for the DREIDING force field tended to be bigger than those for the CVFF(950) force field, probably because of the larger electrostatic interaction. The cell lengths *a* and *b* were more sensitive to the initial guest orientations than was that of *c*. The overall change of *a*/*b* was less than 2−3% with DREIDING and less than 0.2% with CVFF(950). The unconstrained cell angles varied less than 0.4% for both force fields.

The energy minimum for an initial orientation (1) is shown in Figure 1. Other initial orientations gave rise to symmetry-related minima. For each cage, we found six minima that were related by the initial host symmetry. From the results of all MM calculations it follows that the all-trans configuration of the *n*-hexane included molecule, including the position of the methyl deuterons, was the most stable in the Dianin's compound cage. The long molecular axis of *n*-hexane was almost parallel to the crystal *z* axis, and the small tilt of the molecule was dictated by the bulky methyl groups at the center of the cage, as illustrated in Figure 1. This means that the eight methylene deuteron C−D bonds and two of each methyl group's C−D bonds formed an angle of almost 90° with the long molecular axis. The third deuteron of each methyl group then formed an angle of 35.26° with this same axis. On the left side of Figure 2 we show the all-trans *n*-hexane conformation. From this point, all that is described concerning the *n*-hexane methyl deuterons H1, H2, and H3 is valid also for the deuterons H12, H13, and H14.

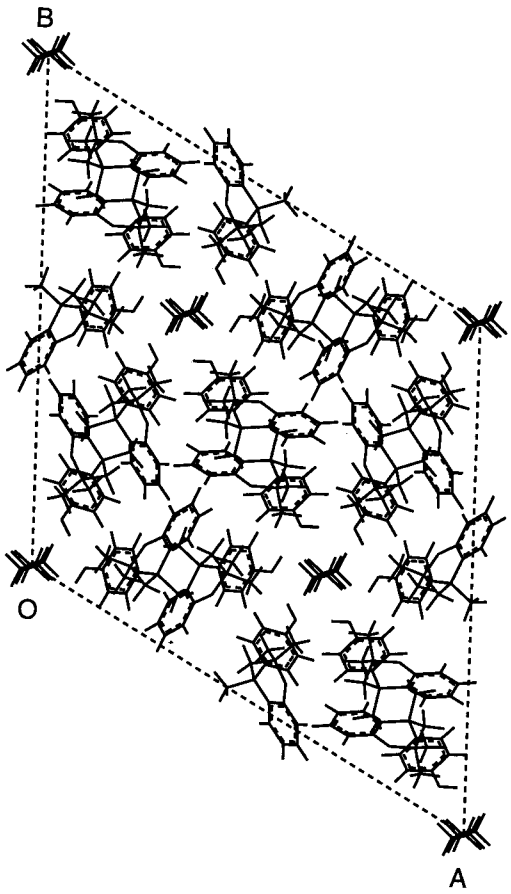

Figure 1. One of the calculated minima of *n*-hexane−Dianin's inclusion compound as viewed from the crystallographic *c* axis as defined in ref 9. Three molecules of the guest per unit cell were considered during the calculation. The hexane molecules were found to be all-trans at the minimum, with the orientation dictated by the host methyl groups at the center of the cage.

MD simulations showed that at high temperatures the molecules jump between three C_3 related sites keeping the all-trans configuration. This can be seen on the left side of Figure 3, which shows data obtained when the directions of the methylene groups were monitored by following the angles between their bisector planes (e.g., the bisector of H4C2H5 is given by the C1C2C3 plane) and a fixed plane in the crystal frame (the *bc* or the *ab* crystal planes, for example). The long molecular axis was, on average, parallel to the crystal *z* axis, which means an average angle of 90° between the methylene C−D bonds and this crystal axis. At low temperatures, we did not observe any jumps on the time scale of the simulation.

The dynamics of the hydrogens in the methyl groups was monitored by observing the torsion angle of one of the hydrogen atoms with respect to the backbone chain. These hydrogens were found to jump between the three sites that are related by the pseudosymmetry axis defined by the methyl carbon−carbon bond (e.g., C1C2), as can be observed on the left side of Figure 4. The jump rates (relative to the chain) were found to be slower than the 3-fold jumps experienced by the chain, and these jumps were not observed at low temperature.

(34) Seff, K.; Shoemaker, D. P. *Acta Crystallogr.* **1967**, *22*, 162.

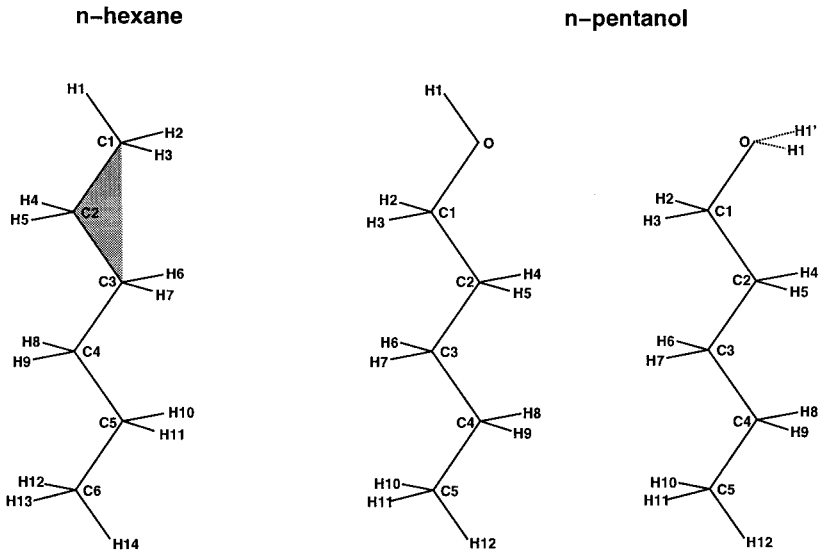

Figure 2. Left: all-trans conformation of the *n*-hexane molecule. Plane C1C2C3 that bisects H4C2H5 is hatched. Center: all-trans conformation of the *n*-pentanol molecule. Right: gauche$^+$ and gauche$^-$ conformations of the hydroxyl group of *n*-pentanol.

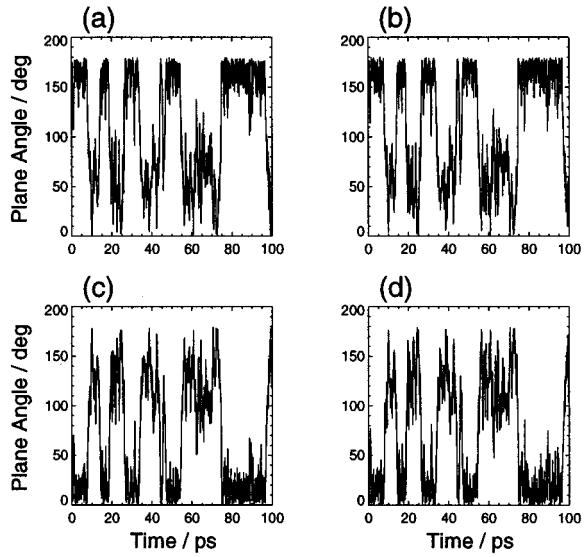

Figure 3. We monitored the angles of planes C1C2C3 (a), C3C4C5 (b), C2C3C4 (c), C4C5C6 (d) with the crystallographic *bc* plane. The C_3 related orientations showed up at ∼160°, ∼40°, ∼80° (since the angles ∈ [0°,180°], the expected 40° − 120° = −80° value was "reflected" back to +80°). The all-trans character is inferred from the evident symmetry between (a), (b), (c), and (d).

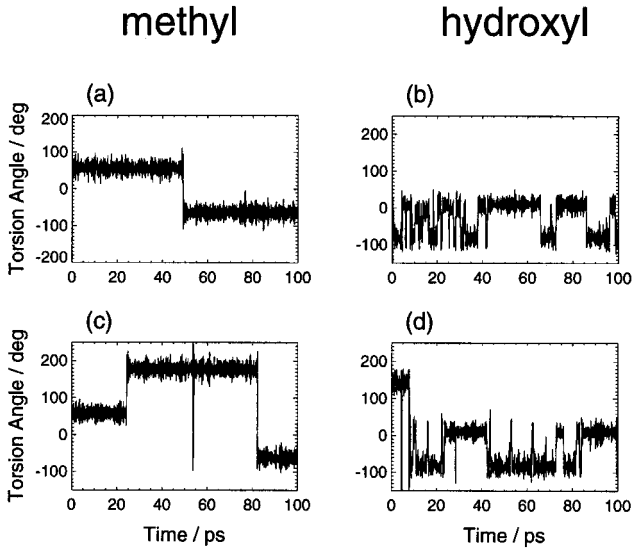

Figure 4. Left side: torsion angle of two methyl group deuterons (e.g., H1C1C2H4) as a function of time in the MD simulation; (a) went only through two of three possible conformations; (c) experienced all the three. Right side: torsion angle of two hydroxyl group deuterons (e.g., H1OC1H2) as a function of time in the MD simulation; (b) started at gauche and changed only from gauche$^+$ to gauche$^-$; (d) started as trans and rapidly went to gauche, as in (a).

3.2.2. *n*-Pentanol−Dianin's Compound. For the pentanol guest molecule, the minimizations with the two different force fields showed slightly different results, as for the hexane. The overall change in *a*/*b* was less than 2−3% with DREIDING and less than 0.1% with CVFF(950). The unconstrained cell angles also varied by less than 0.4% for both force fields.

The calculated energy minima were very similar to those of the hexane, with a slightly bigger tilt angle of the molecular long axis with respect to the crystal *z* axis. The choice to put one of the pentanol molecules in an "upside down" position (that is, with respect to the other two included pentanol molecules) gave the same results as above, both from the point of view of the structure of the guest molecule and from its energy values.

From the MM calculations it follows that there were three stable configurations of the *n*-pentanol molecule (with approximately the same total energy), all with an all-trans conformation of the carbon chain. In the first, the hydroxyl group pointed in the trans direction, approximately parallel to the C1−C2 bond. The other two can be obtained by a rotation of approximately 120° of the hydroxyl group around the O−C1 bond (gauche$^+$ and gauche$^-$ conformations, g$^+$ and g$^-$). In both cases the methylene and methyl C−D bonds formed the same angles with the long molecular axis those as described before for the *n*-hexane guest molecules. This is shown on the right side of Figure 2.

The MD simulations showed that the hydroxyl deuteron, already at low temperatures, surprisingly adopts only the two conformations of the second type described above (g$^+$ and g$^-$). Fast jumps were observed between the g$^+$ and g$^-$ conformations. All pentanol molecules that were initially in the all-trans conformation found their way very quickly to one of the gauche configurations. This is shown on the right side of Figure 4.

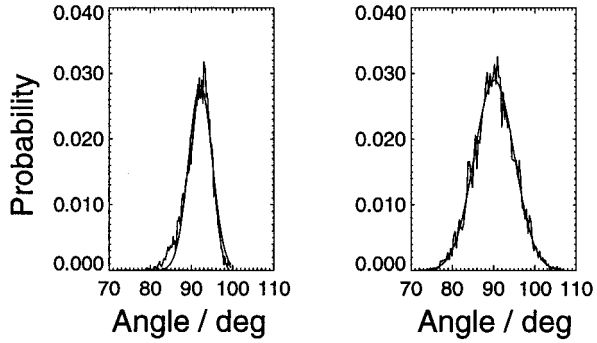

Figure 5. Distribution of angles that the methylene bisector plane C1C2C3 of *n*-pentanol formed with respect to the crystallographic *ab* plane in Dianin's inclusion compound. Calculated at 77 K (right) and 300 K (left), from MD trajectories of 100 ps.

Table 4. Standard-Deviation Values for the Angle between Guest Methylene Groups Bisector Planes and Molecular Crystal Planes after Fitting the Angular Distribution to a Gaussian Shape[a]

	angle with plane *ab*/deg		angle with plane *bc*/deg	
molecule	LT (77 K)	RT (300 K)	LT (77 K)	RT (300 K)
pentanol	3	5	9	15
hexane	2	4	8	16

[a] The values are an average of the angles between the different molecular bisector planes and the crystallographic *ab* and *bc* planes.

Furthermore, the MD simulations showed that at high temperatures the molecules jump between the three C_3 related sites, while keeping the all-trans configuration for the carbon chain (C1 to C5). The methyl group also behaved similarly to those of *n*-hexane. At low temperature no motions of the methyl group or the whole molecule were observed.

3.2.2.b. Librational Motions of Guests in Dianin's Compound. The librational motions of the methylene bisector planes of hexane and pentanol were monitored relative to the crystal *bc* and *ab* planes. In Figure 5 we show the distribution of angles of one of the methylene bisector planes of a *n*-pentanol molecule for the whole simulation period.

We fitted the distributions to a Gaussian line shape, thus obtaining a standard-deviation value for each plane angle with respect to the crystal planes at the different temperatures. The average of these standard-deviation values for all bisector planes in the included molecules is given in Table 4.

3.2.3.a. *n*-Hexane−Zeolite 5A. The minimization of the host−guest structure for the zeolite systems showed that the potential experienced by the guest molecules was shallower than that experienced for Dianin's compound. This is because of the absence of steric barriers that exist in Dianin's compound. Only at the proximity of the zeolite cage walls did we observe a drop in the interaction energy of the guest with the host.

The variations of the unconstrained host framework cell parameters were also found to be much smaller than those for the Dianin's compound crystal, as dictated by the Burchard−DREIDING force field. The minimized structures with only one guest included per unit cell gave the minimum-energy positions of these guest molecules.

The MM calculations showed that the *n*-hexane molecules were located close to the wall of the zeolite cavity (S4R windows) and that their minimum energy conformation was again all-trans with the bulky methyl groups pointing in the directions of two of the S8R windows. There were 12 such sites in each cage, one of which is shown in two different views in the Figure 6.

The presence of a guest in the neighboring cages influenced the MM calculations. Since the difference in energy between an unbound and the bound guest molecule is small, the minimizing algorithm preferred to keep all guests in an ordered arrangement, avoiding interactions that could arise from having two hexane molecules bound to close-by walls of the zeolite.

The MD at high temperatures indicated that the *n*-hexane molecules tend to keep their all-trans conformations. This can be seen in Figure 7, which shows the data obtained when the directions of the methylene bisector planes were monitored. As explained before for the Dianin's compound, this can be visualized by the fact that the relative orientations of the C1C2C3 and C3C4C5 planes did not change during the overall motion of the molecule (as well as the C2C3C4 and C4C5C6 planes). In this case though, the overall motion did not exhibit 3-fold symmetry. The positions of the center of gravity of the guest molecules showed that some of the molecules were able to move from one minimum-energy position to another. No evidence was found for guest molecules diffusing from one cage to a neighboring cage.

At high temperature, the methyl groups showed 3-fold jumps of their deuterons relative to the whole molecule. This motion

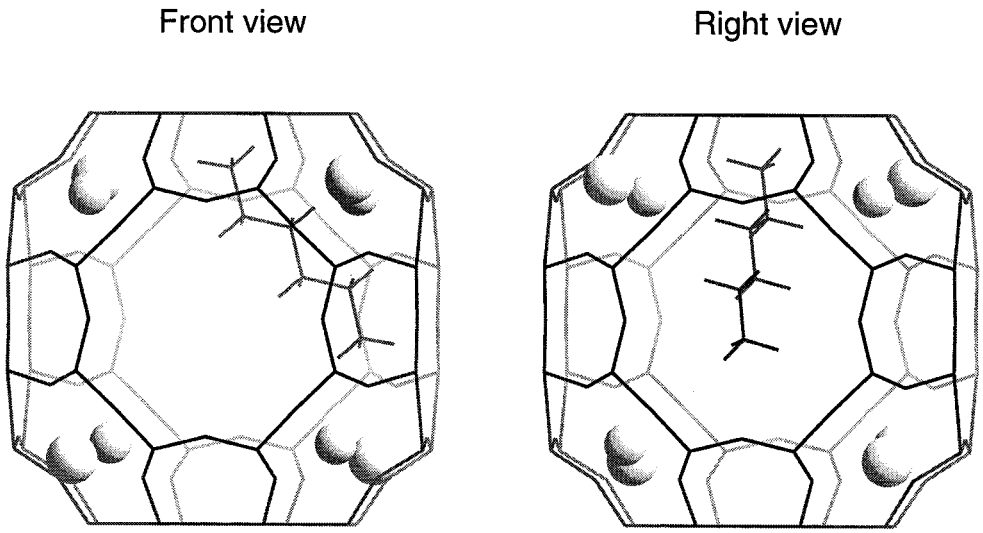

Figure 6. Front and left view of one of the minimum-energy structures of the *n*-hexane−zeolite 5A inclusion compound. Note the bulky methyl groups pointing in the direction of the α cages S8R windows and the proximity of the chain to the S4R window.

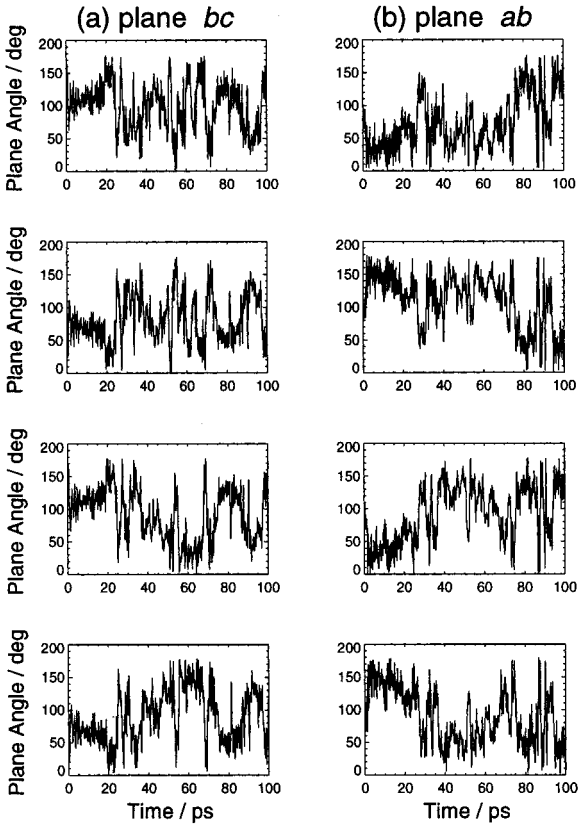

Figure 7. We monitored the angles of planes (top to bottom) C1C2C3, C2C3C4, C3C4C5, and C4C5C6 with the crystallographic *ab* (a) and *bc* (b) planes. The all-trans character is inferred from the evident symmetries in (a) and (b). The absence of correlation between (a) and (b) showed that the motion is essentially isotropic.

and the others mentioned above were not observed at the low-temperature simulations. MD calculations performed with the minimized structure of one or eight guests per zeolite unit cell gave the same overall behavior.

3.2.3.b. *n*-Pentanol−Zeolite 5A. The MM calculations for the *n*-pentanol molecule showed that this guest molecule also has an energetically preferred all-trans conformation, including the hydroxyl group. Its overall position is the same as that for the *n*-hexane molecule with the hydroxyl deuterons pointing in the direction of one of the oxygen atoms of the S8R window. We should point out that for most (but not all) of the minimized structures, the energy of the bound *n*-pentanol molecule was lower than that of the bound *n*-hexane.

The MD calculations showed that at low temperatures the hydroxyl groups jumped back and forth from the trans to the gauche conformations. At the low temperature no motions of the carbon chain or the methyl group deuterons were observed.

At the high temperature the configuration of the carbon chain remained all-trans, while the fluctuations of the directions of the C*i*C*j*C*k* planes were somewhat slower than for *n*-hexane. This can be a result of the "chemical anchoring" of the hydroxyl group to one of the framework oxygen atoms common to S4R and S8R windows. Indeed, for the *n*-pentanol guests we observed much less motion of the molecules between minimum-energy positions than was observed for *n*-hexane. The methyl group reorientation rates were approximately the same as those for *n*-hexane.

No evidence was found for guest diffusion between cages for either of the simulations, with one guest or eight guests per unit cell.

3.3. Conclusions of MM and MD Calculations. Here we summarize the results of the MM and MD calculations that are relevant for the analysis of the ^{2}H NMR spectra.

3.3.1. Molecular Mechanics Calculations (Energy Minimization). The Dianin's compound imposes its intrinsic symmetry onto the guests. Their minimal-energy positions are determined mostly by the repulsion term of the potential-energy function. The methyl groups of the host molecules, which point in the direction of the center of the cage and give it its hourglass shape, defined these minima. Small deformations of the cages from the unsolvated structures were observed, depending on the guest position. The major finding for the Dianin's inclusion compound were the following:

(i) The carbon chains of the guest molecules were in their all-trans conformation at the minimum-energy positions.

(ii) The hydroxyl groups of the pentanol molecules had three different minimum-energy positions, with trans, g^+, and g^- conformations with respect to the carbon chain.

For the zeolite 5A cage, the minima of the guest molecules were very well defined and very similar for the two guest molecules.

(iii) Both *n*-hexane and *n*-pentanol remained in their all-trans conformations at these minima, close to the wall of the α cage, with the head and tail of the chains pointing in the direction of the S8R windows between the α cages.

(iv) In the case of *n*-pentanol, the hydroxyl group of the alcohol molecules interacted strongly with one of the framework oxygen atoms common to the S8R and S4R windows.

3.3.2. Molecular Dynamics Calculations (Time Evolution). MD simulations were applied to the minimized structures of the host−guest systems for 20−100 ps at two different temperatures. The high (300 K) and low (77 K) temperature MD calculations for the Dianin's inclusion compounds gave the following results.

(v) In the Dianin's compounds, both guests maintained their all-trans conformation throughout the simulation and jumped between the C_3-symmetry-related minima dictated by the host symmetry. For each molecule a few jumps (up to several tens) during the simulation at 300 K were observed. This corresponds to a jump rate on the order of $10^{10}-10^{12}$ s^{-1}.

(vi) In addition to this motion, the hydrogen atoms of the methyl groups permuted as dictated by their own 3-fold pseudosymmetry. This process was slower than the overall reorientational motions of the chains about their long molecular axes (we observed not more than 10 methyl group jumps for any single molecule).

(vii) For the hydroxyl groups of the pentanol guests, the hydrogen atoms adopted preferentially the gauche conformations and exhibited a jump process between the g^+ and g^- conformations. This process was faster than the jumps of the molecule about its long axis and the jumps of the hydrogen atoms in the methyl groups. This was also the only motion observed at the low-temperature calculations.

MD simulations for the zeolite 5A showed the following:

(viii) The guests maintained on average their all-trans conformation. Guest molecules moved between minima and reoriented more isotropically than in Dianin's compound. The overall reorientation of the guest molecules with respect to the framework was slower for the *n*-pentanol than for the *n*-hexane guests.

(ix) Methyl groups of both guests experienced the same motion as described in (v).

(x) The hydroxyl group hydrogen atoms of the pentanol guest jumped between the three possible conformations (trans, g^+,

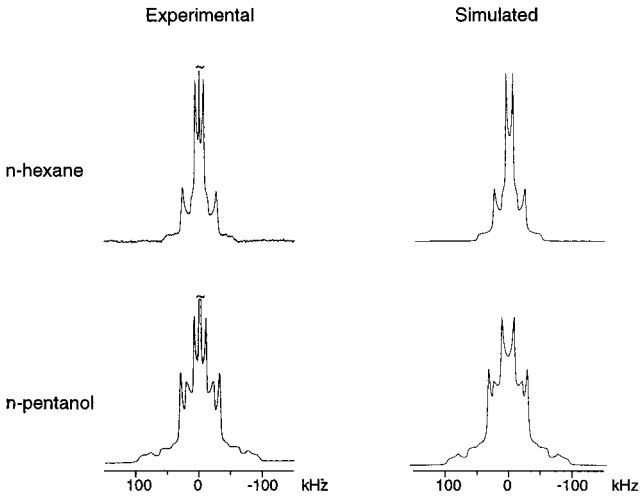

Figure 8. Experimental (300 K) and simulated ^{2}H NMR spectra of d_{12}-*n*-pentanol and d_{14}-*n*-hexane in their Dianin's inclusion compounds.

and g$^-$) even at low temperatures. No additional internal motions were observed at low temperatures.

Temperature-dependent librational motions were observed for all above-described dynamic processes. They were on the same order of magnitude for the Dianin's and zeolite 5A inclusion compounds. Gaussian fitted line shapes enabled us to calculate the standard deviations of the libration angles.

(xi) In the case of Dianin's compounds, the libration angle perpendicular to the long axis varies from 8−9° at 77 K to 15−16° at 300 K, and the libration angle parallel to the same axis varies from 2−3° at 77 K to 4−5° at 300 K.

4. NMR Results

4.1. *n*-Hexane−Dianin's Compound. The results of our MM and MD calculations predicted an all-trans *n*-hexane rotating about its long molecular axis [(i) and (v)]. The fast C_3 reorientation of an all-trans deuterated hexane molecule reduces its effective nuclear quadrupolar coupling constant NQCC (and thus the quadrupolar splitting) by a factor

$$R(\theta) = {}^1/_2(3\cos^2\theta - 1)$$

where θ is the angle between the C−D bond direction and the long rotational axis of the molecule. In reference to Figure 2, the reduction factors for the methylene and methyl deuterons are

$$R(\text{methylene}) = R(\text{methyl H2,H3}) = R(90°) = -{}^1/_2$$

$$R(\text{methyl H1}) = R(35.26°) = {}^1/_2$$

Since the deuterium NMR spectrum is intrinsically symmetric, we cannot differentiate between these two types of deuterium spectra.

The MD also showed a C_3 reorientation [(vi)] of the methyl groups deuterons that permutes H1,H2, and H3, reducing the deuterium quadrupolar coupling constant by

$$R(\text{methyl H1,H2,H3}) = R(70.5°) = {}^1/_3$$

The spectrum of d_{14}-*n*-hexane in Dianin's compound at room temperature is shown on the upper left side of Figure 8. This spectrum is a clear superposition of several powder patterns belonging to the different deuterons of the molecule. We can observe three distinct patterns; the first is a sharp line at zero frequency that originates from a small fraction of the deuterium nuclei that reorient very fast in the sample, and the other two are axially symmetric powder patterns with reduced quadrupolar splitting. The quadrupolar splitting of the *inner* shape in the spectrum is 13.5 kHz and that of the *outer* shape is 53.7 kHz, as determined by the line shape simulation on the upper right side of Figure 8.

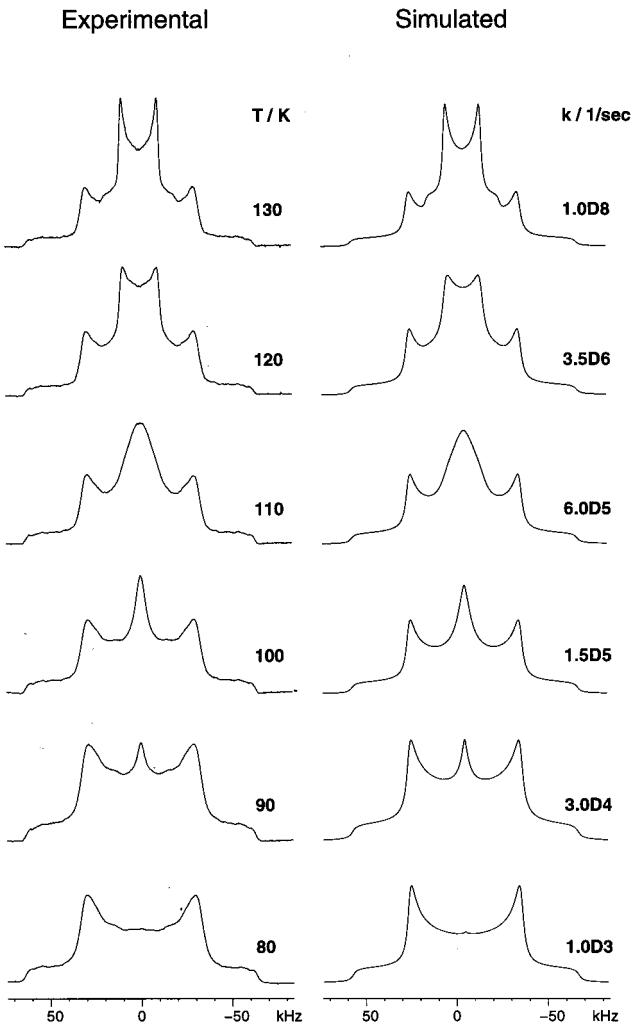

Figure 9. Experimental and simulated ^{2}H NMR spectra of d_{14}-*n*-hexane−Dianin's inclusion compound. Left: experimental spectra and temperatures. Right: simulations of the methyl motion and fitted jump rates of the methyl deuterons reorientation around their pseudosymmetry axis.

The experimental temperature-dependent spectra of d_{14}-*n*-hexane in Dianin's compound are shown in Figure 9. As we lowered the sample temperature to about 150 K, the two powder patterns showed only a small increase in their quadrupolar splittings (the *inner* increased to 14 kHz and the *outer* to 54 kHz). The intensity of the sharp line at zero frequency diminished, and at 130 K it completely disappeared. Below 130 K the *inner* and *outer* powder patterns showed different behaviors. The *outer* powder pattern continued to increase its quadrupolar splitting, while the *inner* one showed a change in its line shape. This is an indication that the correlation rates of the dynamics experienced by *inner* deuterons become on the order of their quadrupolar coupling constants. The *inner* spectrum broadened, and the splitting observed at 130 K (20 kHz) gave way to a broad line with a width of 22 kHz at 110 kHz, which decreased in intensity and disappeared. The *outer* spectrum had a quadrupolar splitting of 61 kHz at 80 K.

The observed NMR spectra are in complete agreement with the predicted dynamic model. At 80 K a single spectrum, with a quadrupolar splitting which is $^1/_2$ the characteristic value of 125 kHz of a static aliphatic deuteron powder pattern, was observed. The process that causes this reduction of the widths of the line shape [(v), motion 1] is in its fast limit and does not affect the spectrum line shape at this or higher temperatures. Indeed, the *outer* spectrum, related to the methylene deuterium nuclei, did not change its line shape from 80 K up to room temperature. Above 80 K, the methyl deuterons experienced a 120° jump process about their pseudosymmetry axis [(vi), motion 2]. This motion affected the line shape of the *inner* spectrum until it reached its fast limit at 130 K. The rates of the jumps (relative to the frame of the molecule) describing motion 2 are shown on the right side of Figure 9.

Since motion 2 reached its fast limit at a higher temperature than motion 1, we conclude that motion 2 *must* be slower than motion 1, exactly as predicted from the MD calculations [(vi)].

The MD calculations also indicated the presence of fast small reorientational motions of the guest as well as of the host atoms [(xi)]. The fast librations of the C−D bonds of hexane caused a reduction of their effective quadrupolar coupling constants. An increase of the libration amplitudes at high temperatures resulted in a temperature-dependent decrease of the coupling constants. These librational modes seemed to exist in all directions with different amplitudes and were observed as a reduction of the quadrupolar splitting in the methylene deuterium spectra. This issue will be discussed further after the next paragraph.

4.2. *n*-Pentanol−Dianin's Compound. The results of the MM and MD calculations predicted an all-trans *n*-pentanol, rotating about its long molecular axis [(i) and (v)], just as in the case of *n*-hexane. They also predicted the motions of the methyl deuterons and the hydroxyl deuteron relative to the molecular frame [(vi) and (vii)].

To analyze the deuterium spectra, we assumed that the hydroxyl groups follow a combination of two-site jumps between g^+ and g^- [(vii), motion 3] and three-site jumps of the whole chain around its long molecular axis [(v), motion 1]. Our MD calculations gave us the (average) values of the angles necessary for the analysis. The MD values for these angles were the following: for the two-site jumps between the g^+ and g^- conformations a jump angle of 95° and for the three-site jumps an angle of 100° between the O−D bond and the axis of rotation of the whole molecule.

The room-temperature spectrum at the bottom left side of Figure 8 can be described as follows. The outermost components at ±93.7 and ±77.6 kHz clearly belong to a static hydroxyl group deuteron, with a characteristic large NQCC = 228.4 kHz and an asymmetry parameter $\eta = 0.1$. The parallel components at ±171.3 kHz were very much attenuated by the finite pulse length and are not shown in the figure. This value of the quadrupole coupling constant is much larger than that characteristic of aliphatic deuterons (≈166.7 kHz).

Nevertheless, to eliminate the possibility that the observed features in the room temperature spectrum of *n*-pentanol were actually a superposition of different molecular species, we included a pentanol molecule in Dianin's compound, specifically deuterated at the α methylene positions. Its temperature-dependent spectra showed that there is only one type of included guest.

Three other powder patterns with different quadrupolar splittings of 58.2, 40.8, and 17.8 kHz, which are axially symmetric, are observed in Figure 8. A center line with Lorenzian line shape was also observed corresponding to isotropically reorienting deuterons.

As for the *n*-hexane guests in Dianin's compound, the powder patterns with splittings of 58.2 and 17.8 kHz correspond to the methylene and methyl deuterons, respectively, rotating around their symmetry directions and indicating the overall motion of the molecules. Since the $\eta = 0.1$ hydroxyl deuteron spectrum belongs to static deuterons, it must come from the host crystal. Presumably, some deuterium exchange occurred between the hydroxyl groups of host and guest during the preparation of the inclusion compound. The remaining axially symmetric spectrum with splitting of 40.8 kHz could be simulated assuming a combination of motion 1 and motion 3, starting with a typical static powder line shape for a hydroxyl group deuteron, with the experimental measured values of NQCC = 228.4 kHz and $\eta = 0.1$. The simulated spectrum of d_{12}-*n*-pentanol is shown on the bottom right side of Figure 8.

When the temperature was reduced, the hydroxyl deuterium spectrum decreased in intensity and below 200 K it could not be observed. The observed spectra of the methylene and methyl components were very similar to those presented for the hexane guests.

4.3. Libration Motion of the Guest Molecules. In addition to the three types of motion shown above, both *n*-hexane and *n*-pentanol molecules experienced librational motions [(xi)]. These motions caused a reduction of the quadrupolar coupling constant, and we expect the reduction to be more pronounced for the *n*-hexane than for the *n*-pentanol guests.

The reduction of the quadrupolar interaction due to these librations can be estimated using the theoretical models introduced by Hisrchinger and English.[35] Following the derivation of Wittebort et.al.,[36] we call the polar angles of the unique principal axis of the EFG tensor θ_{lib} and ϕ_{lib} and the standard deviations of the Gaussian distribution for these two polar angles $\Delta\theta_{lib}$ and $\Delta\phi_{lib}$. Upon consideration of an axially symmetric tensor and small-angle fluctuations, ($\Delta\theta_{lib}^2$ and $\Delta\phi_{lib}^2 \ll 1$) the reduced principal eigenvalues of the EFG tensor are given by[36]

$$V_1^* = \frac{1}{2}(eq)(3\Delta\phi_{lib}^2 - 1), \quad V_2^* = \frac{1}{2}(eq)(3\Delta\theta_{lib}^2 - 1), \quad \text{and}$$

$$V_3^* = \frac{1}{2}(eq)(2 - 3\Delta\phi_{lib}^2 - 3\Delta\theta_{lib}^2)$$

From our MD simulations we estimated the standard deviations of the average libration angles (see Table 4) for the bisector plane of the methylene guest molecules with respect to two different crystal planes at high and low temperatures. The average relative reduction *R* of the coupling constants at 77 and 300 K can be evaluated by

$$R = \text{NQCC (300 K)/NQCC (77 K)}$$

The experimental values of these reductions were obtained from the quadrupolar splitting of the methylene deuteron spectra.

Table 5 shows that the predicted reductions are in good quantitative agreement with the measured ones.

4.4. *n*-Hexane−Zeolite 5A. The MM and MD calculations predicted that the *n*-hexane guest molecules stay in their all-trans conformation with well-defined minimum-energy positions close to the wall of the α cage [(iii)]. In addition, they experienced a rather isotropic reorientation process at high

(35) Hirschinger, J.; English, A. D. *J. Magn. Reson.* **1989**, *85*, 542−553.

(36) Wittebort, R. J.; Olejniczak, E. T.; Griffin, R. G. *J. Chem. Phys.* **1987**, *86*, 5411−5420.

Table 5. Reduction of the Quadrupolar Interaction Due to Rapid Librations, Following the Model of Hirschinger and English[35a]

molecule	calculated reduction (%)	NMR measured reduction (%)
pentanol	92	94
hexane	90	88

[a] The NMR reductions were measured from the quadrupolar splitting of the methylene deuteron spectra.

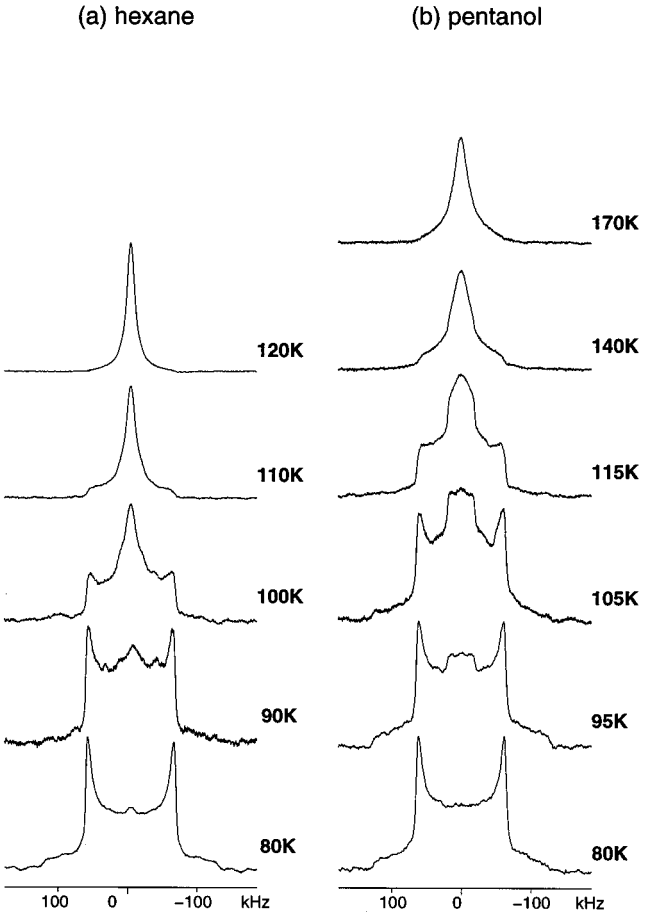

Figure 10. Experimental ^{2}H NMR spectra of d_{14}-*n*-hexane (left) and of -*n*-pentanol (right) adsorbed in zeolite 5A.

temperature [(viii)] at which the chain is able to move between these minima.

The ^{2}H NMR results of the perdeuterated *n*-hexane are shown on the left side of Figure 10. The spectrum of *n*-hexane at 80 K has the shape of a static powder pattern, with a characteristic splitting of 124 kHz between its sharp perpendicular components. The fact that all deuterons were static at this temperature, including the methyl groups, is in perfect agreement with the strong interactions calculated between the host and guest atoms [(iii)], and with the results of the MD calculations [(x)].

As the temperature was raised to 100 K, we observed a spectrum that is a superposition of two spectral components. Apart from the components at ±62 kHz, we observed sharp features with a splitting of 70−75 kHz and a central peak with a 30 kHz width. The τ dependent spectra in the range 90−100 K suggests that these features are related to methyl group dynamics, but they are not enough defined to allow us to simulate the experimental line shapes.

Above 120 K the spectrum became a single Lorenzian line, with a line width that decreased from 12.5 kHz at 120 K to 5 kHz at 200 K. At higher temperatures the spectra became even narrower. This is an experimental indication of the high degree of spatial reorientation expected from the MD calculations [(viii)].

4.5. *n*-Pentanol−Zeolite 5A. MM and MD calculations for the *n*-pentanol guest molecules show that they were also in the all-trans conformation, with well-defined minima close to the wall of the α cage [(iii)] and that they experienced an isotropic reorientation process [(viii)] at high temperatures. In addition, the calculations predicted that the *n*-pentanol experiences a stronger interaction with the cage atoms than the *n*-hexane functional groups. This interaction slows down the reorientational motion for the pentanol when compared to the *n*-hexane guest molecule [(viii)]. The hydroxyl groups are expected to jump between all three possible conformations even at low temperatures [(iv)] and [(x)].

The ^{2}H NMR results of the perdeuterated *n*-pentanol in zeolite 5A are shown on the right side of Figure 10. At low temperatures the experimental NMR spectra of *n*-pentanol resemble those of the *n*-hexane molecules in zeolite 5A.

The spectrum of *n*-pentanol included in zeolite 5A at 80 K is a static powder pattern with the characteristic quadrupolar splitting of 125 kHz. The hydroxyl deuteron signal was not observed, which can be caused by an intermediate rate of the g^+-g^- exchange process described in [(x)] or by long spin−lattice relaxation effects.

At 100 K the spectrum is composed of two components, like in the case of *n*-hexane: a central component with sharp features at ±38 kHz and a center peak with a width of 36 kHz, which is very characteristic for the reorientation of methyl deuterons about their C_3 pseudosymmetry axis. The outer part of the spectrum was the same as the static powder spectrum observed at lower temperatures. When the temperature was raised to 120 K, the static component of the spectrum lost intensity, while the central component gained intensity. This component not only had contribution from the rapidly reorienting methyl deuterons but also had contribution from the other deuterons, which were static at lower temperatures. The central portion of the spectrum became even more enhanced at 160 K, while the static components got even weaker. At this temperature we observed sharp features at ±60 and ±32.5 kHz and a center peak with a 36 kHz width. Further elevation of the temperature made the spectrum simpler, showing a single Lorenzian line that had a width of 22 kHz at 200 K. The motions causing this change in line shapes must be related to the reorientation of methyl groups and to a fraction of molecules for which the methylene groups were also able to reorient.

Because of the high complexity of the motion at the intermediate temperatures, it is not justified to try to simulate these spectra. As the temperature was raised, the width of the central line reduces further, but it remains always broader than the equivalent line in the *n*-hexane spectrum. This is an indication of the more restricted motion of the *n*-pentanol molecule as compared with the *n*-hexane molecules [(viii)].

4.6. Spin−Lattice Relaxation. Spin−lattice (T_1) relaxation times were also measured for the different spectral components of the guests in Dianin's inclusion compound and zeolite 5A at different temperatures. The T_1 values of the perpendicular components of the methylene spectra are shown in Figure 11. In the case of the guest molecules in Dianin's compound we can assume that the 3-fold jumps of the whole chain are the only source of T_1 relaxation of the methylene deuterons. Then the correlation times of this motion at its fast motional limit can be evaluated using $1/T_1 = \omega_Q^2\tau_c/4$ for the perpendicular

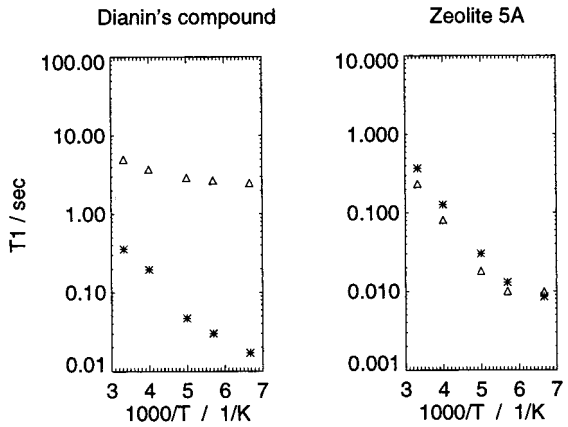

Figure 11. Spin−lattice relaxation times of methylene deuterons of guest in Dianin's compound (left) and in zeolite 5A (right). Circles represent *n*-hexane methylene deuterons, and asterisks represent the *n*-pentanol methylene deuterons.

components of the methylene spectra. At room temperature the rate obtained from the fitted correlation times τ_c was approximately $10^{10}-10^{11}$ s^{-1}, in very good agreement with the rates estimated from the MD simulations in [(v)].

5. Summary

We present a study of host−guest interactions in inclusion compounds. Two guests of approximately the same size but different chemical character were used, *n*-hexane and *n*-pentanol. These two molecules were included in an organic (Dianin's compound) and an inorganic (zeolite 5A) host. Molecular mechanics and molecular dynamics simulation methods were applied to the different host−guest systems, resulting in the minimum-energy structures of the inclusion compounds, and their dynamics behavior at different temperatures. These results enabled us to propose models for the structure and dynamics of these systems. The structure and dynamics of the guest molecules in the organic and inorganic inclusion compounds were probed by solid-state NMR. The ^{2}H NMR temperature-dependent spectra were analyzed and compared to the results of molecular modeling calculations, showing a very high degree of agreement.

There is a clear advantage of proposing and checking structural and dynamic models (derived from molecular modeling calculations) for solid-state NMR line shape analysis in terms of molecular reorientation, chemical exchange processes, and correlation times. The availability of sophisticated but easy-to-use software packages such as MSI's Cerius^2 facilitates the task of molecular modeling for the spectroscopist. This approach can help provide a more correct visualization and understanding of the molecular structure and dynamics as studied by solid-state NMR.

Acknowledgment. We acknowledge Mr. Koby Zibzener from the Electronics Workshop and Mr. Reuven Dagan from the Mechanics Workshop for their help with the building of the low-temperature ^{2}H NMR probe. We also thank Prof. Ulrich Haeberlen and Dr. Peter Speier from the Max-Plack-Institut für Medizinische Forschung at Heidelberg for fruitful discussions in the early stages of this project.

JA980831T